Retinal Nonperfusion Relationship to Arteries or Veins Observed on Widefield Optical Coherence Tomography Angiography in Diabetic Retinopathy

Akihiro Ishibazawa,[1,2] Lucas R. De Pretto,[3,4] A. Yasin Alibhai,[1] Eric M. Moult,[3] Malvika Arya,[1] Osama Sorour,[1] Nihaal Mehta,[1] Caroline R. Baumal,[1] Andre J. Witkin,[1] Akitoshi Yoshida,[2] Jay S. Duker,[1] James G. Fujimoto,[3] and Nadia K. Waheed[1]

[1]New England Eye Center, Tufts Medical Center, Boston, Massachusetts, United States
[2]Department of Ophthalmology, Asahikawa Medical University, Asahikawa, Japan
[3]Department of Electrical Engineering and Computer Science, and Research Laboratory of Electronics, Massachusetts Institute of Technology, Cambridge, Massachusetts, United States
[4]Nuclear and Energy Research Institute, Sao Paulo, Sao Paulo, Brazil

Purpose. To evaluate whether retinal capillary nonperfusion is found predominantly adjacent to arteries or veins in eyes with diabetic retinopathy (DR).

Methods. Sixty-three eyes from 44 patients with proliferative DR (PDR) or non-PDR (NPDR) were included. Images (12×12-mm) foveal-centered optical coherence tomography (OCT) angiography (OCTA) images were taken using the Zeiss Plex Elite 9000. In 37 eyes, widefield montages with five fixation points were also obtained. A semiautomatic algorithm that detects nonperfusion in full-retina OCT slabs was developed, and the percentages of capillary nonperfusion within the total image area were calculated. Retinal arteries and veins were manually traced. Based on the shortest distance, nonperfusion pixels were labeled as either arterial-side or venous-side. Arterial-adjacent and venous-adjacent nonperfusion and the A/V ratio (arterial-adjacent nonperfusion divided by venous-adjacent nonperfusion) were quantified.

Results. Twenty-two eyes with moderate NPDR, 16 eyes with severe NPDR, and 25 eyes with PDR were scanned. Total nonperfusion area in PDR (median: 8.93%) was greater than in moderate NPDR (3.49%, $P < 0.01$). Arterial-adjacent nonperfusion was greater than venous-adjacent nonperfusion for all stages of DR ($P < 0.001$). The median A/V ratios were 1.93 in moderate NPDR, 1.84 in severe NPDR, and 1.78 in PDR. The A/V ratio was negatively correlated with the total nonperfusion area ($r = -0.600$, $P < 0.0001$). The results from the widefield montages showed similar patterns.

Conclusions. OCTA images with arteries and veins traced allowed us to estimate the nonperfusion distribution. In DR, smaller nonperfusion tends to be arterial-adjacent, while larger nonperfusion tends toward veins.

Keywords: diabetic retinopathy, optical coherence tomography, retinal ischemia, retinal artery, retinal vein

Diabetic retinopathy (DR) is among the leading causes of blindness worldwide,[1] and is characterized by structural and functional alterations of the retinal microcirculation. Retinal ischemia is one of the central underlying disease processes related to the progression of DR and is partly caused by retinal capillary nonperfusion due to either intraretinal capillary occlusion or capillary dropout. This retinal ischemia results in impaired oxygenation of the metabolically demanding retinal neurons as well as increased generation of proangiogenic agents such as vascular endothelial growth factor (VEGF).[2] Therefore, studying the features of retinal ischemia is essential in understanding the etiology of the microvascular damage in DR.

Several reports emphasize that "arterial-side" vascular impairment plays a critical role in the progression of pathologic diabetic lesions.[3–9] Histology studies by Ashton[3] showed a periarteriolar distribution of the vascular lesions in DR and the progression of capillary closure from the arterial side.[3] Moreover, even in early diabetic microvascular changes, Stitt and colleagues[6–9] demonstrated that the thickening of the capillary basement membrane in the arterial side was greater than that in the venous side, and that microaneurysms and acellular capillaries were predominantly distributed on the arterial side. These studies were mostly qualitative assessments in postmortem eyes; therefore in vivo quantitative approaches could generate broader insights into the pathogenesis and progression of arterial or venous involvement in DR.

The recent clinical adoption of optical coherence tomography (OCT) angiography (OCTA) has provided clinicians with a noninvasive, volumetric modality for visualizing the retinal vasculature at micrometer resolutions.[10,11] In particular, retinal capillary nonperfusion, which appears on OCTA images as

areas of low OCTA signal, is more clearly visualized and demarcated on OCTA than on fluorescein angiography (FA) images.[12] Our group recently quantified retinal capillary nonperfusion, a surrogate for retinal ischemia in DR of different severities, using widefield swept-source (SS)-OCTA.[13] In the current study, we modified this technique and developed a new method for automated visualization and quantification of arterial- or venous-adjacent capillary nonperfusion, assessing growth and enlargement using widefield OCTA.

METHODS

Study Population

This cross-sectional observational study was approved by the Institutional Review Boards at the Massachusetts Institute of Technology and Tufts Medical Center. The research adhered to the Declaration of Helsinki and the Health Insurance Portability and Accountability Act.

We retrospectively identified patients with DR who had undergone widefield OCTA imaging in the retina clinic at New England Eye Center over a 1-year period (between January 2017 and January 2018). As part of their routine care, these patients had undergone comprehensive ophthalmologic examinations, including measurement of best-corrected visual acuity (BCVA), intraocular pressure, slit-lamp biomicroscopy, color fundus photography, structural OCT imaging, and if clinically indicated, FA. DR was diagnosed and classified by two retina specialists (N.K.W. and C.R.B.) according to the International Clinical Diabetic Retinopathy Severity Scale.[14] Visual acuity was measured using a Snellen chart and expressed as the logarithm of the minimum angle of resolution (logMAR). The presence or absence of diabetic macular edema (DME) was determined based on structural OCT findings. In the current study, eyes with mild nonproliferative diabetic retinopathy (NPDR) were excluded from analysis because, while they may contain areas of capillary dropout, these areas were below the detectable threshold of our algorithm. We also excluded eyes with severe media opacities such as severe cataract or vitreous hemorrhage, a history of vitrectomy, other chorioretinal disorders such as age-related macular degradation, or primary retinal artery or vein occlusion. Eyes that had previously been treated with anti-VEGF injections and/or panretinal photocoagulation (PRP) within 3 months were not included.

OCTA Imaging

OCTA images were obtained using a 100-kHz A-scan rate SS-OCTA instrument (Plex Elite 9000; Carl Zeiss Meditec, Inc., Dublin, CA, USA). OCT(A) volumes covering a 12 × 12-mm retinal area (40° field of view) and centered at the fovea were acquired. Each 12 × 12-mm volume consisted of 500 A-scans per B-scan and 500 B-scan locations per volume scan. Two repeated B-scans were obtained at each B-scan position to generate the OCTA images. In a subset of eyes, five OCTA volumes (each 12 × 12 mm) had been acquired at different fixation points: central, superior nasal, inferior nasal, inferior temporal and superior temporal. Montaged images were generated from these five images using built-in software on the instrument.[15] En face OCTA images of the full retinal thickness, generated by automatically segmenting the inner limiting membrane to 70 μm above the retinal pigment epithelium, were used for analyses. OCTA imaging was performed by trained ophthalmic photographers who repeated image acquisitions several times if necessary to ensure that images with good OCT signal penetration (signal strength ≥7)

and minimal motion artifacts were obtained. This protocol is consistent with the standard diabetic imaging protocol at the New England Eye Center.

Identification and Quantification of Capillary Nonperfusion Areas

We used a custom software, written in MATLAB (MathWorks, Natick, MA, USA), to semiautomatically identify nonperfusion areas in the OCTA images. This software has been fully described in a previous study by our group.[13] Briefly, the software employs spatial variance metrics combined with a flooding-based algorithm to locate regions of possible nonperfusion. The user can exclude artifactual areas prior to analysis, as well as manually correct (i.e., excluding and/or adding) the identified segments, reducing potential artifacts. The scan density used in the 12 × 12-mm imaging and widefield montages is too low to resolve individual capillaries in small areas, such as those surrounding the focal avascular zone. Thus, we have defined a threshold minimum area for the algorithm to select, aiming to improve performance reliability. Therefore, for automatic identification purposes, a nonperfusion area was defined as a nonvessel contiguous region composed of ≥250 pixels (∼0.15 mm²). The foveal avascular zone was detected automatically and was excluded manually. The total capillary nonperfusion as a percentage of the total area was computed as:

$$\text{Total percentage of capillary non-perfusion area} = \frac{\text{Sum of non-perfusion area}}{\text{Field-of-view area} - \text{excluded area}} \times 100\%.$$

Tracing of Retinal Arteries and Veins

Using fundus photographs and FA images where available, first- and second-order retinal arteries and veins were identified. OCTA images allowed the visualization of arterial branches, which are clearly distinguishable from veins by the presence of surrounding hypointense areas, representing the capillary-free zone, due to the absence of efferent vessels coming directly out of walls.[16–18] Furthermore, arteries do not cross other arteries, and veins do not cross other veins. Based on these characteristics, arteries and veins were manually traced up to the level of precapillary arterioles and venules. Neovascular tissue was not traced because it does not contribute to the retinal circulation. In a few cases, large arteries or veins were almost completely occluded and therefore were not visualized on the montaged OCTA images. In these cases, we inspected the B-scan and en face structural OCT and corrected the tracing at the level of second-order branches of the arteries and veins (Supplementary Fig.).

Arterial-Adjacent or Venous-Adjacent Capillary Nonperfusion

In order to determine if capillary nonperfusion was adjacent to arteries or veins, the artery-/vein-traced en face OCTA images were used as a guide alongside the automatically identified nonperfusion regions. The vein and artery tracings were exported as separate images, and using custom MATLAB software, were binarized and subjected to a Euclidean distance transformation.[19] After this transformation, each pixel was assigned a value corresponding to its distance from the nearest nonzero element in the image. Two distinct maps were created with values that indicated the nearest artery and vein. Then, for each nonperfusion pixel, the adjacency to the nearest vessel, whether artery or vein, was assigned. In the case of equal
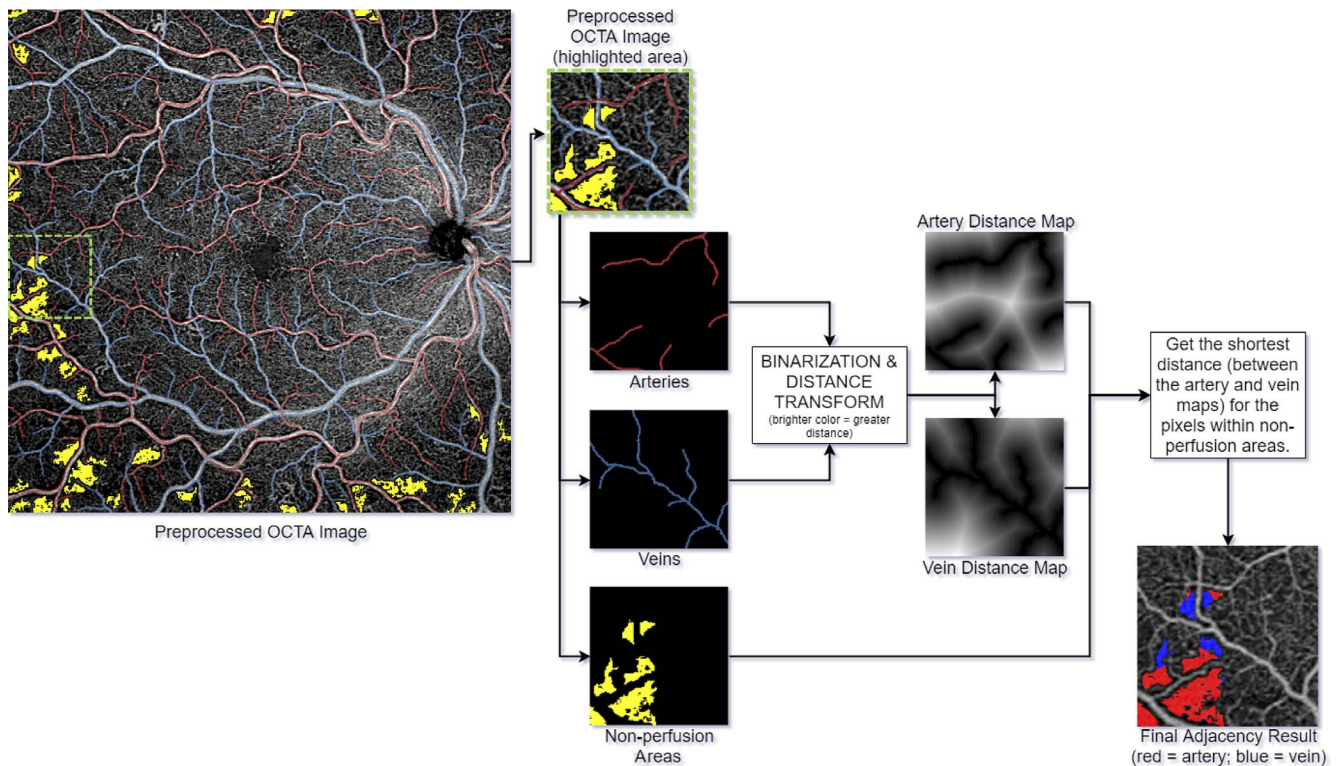
FIGURE 1. Flowchart displaying the steps for assessing nonperfusion adjacency. The OCTA image (*leftmost image*) is preprocessed to have the arteries (*red*) and veins (*blue*) manually outlined, as well as nonperfusion areas (*yellow*) automatically identified. The magnified highlighted region (*green dashed box*) is used as an example. The masks for nonperfusion, arteries, and veins are separated. The latter two are binarized and undergo a distance transform, creating the distance maps. Those are used in conjunction with the nonperfusion mask, where nonperfusion areas are classified as arterial-adjacent or venous-adjacent based on the shortest distance. Finally, a false-color map is overlaid on the original OCTA image.

distances, the adjacency was randomly assigned. Finally, a false-color image was generated for visualization purposes (red: arterial side; blue: venous side). The values for nonperfusion adjacency were defined as the percentage of nonperfusion adjacent to the arterial side (arterial-adjacent nonperfusion) and the percentage of nonperfusion adjacent to the venous side (venous-adjacent nonperfusion). Arterial-adjacent nonperfusion divided by venous-adjacent nonperfusion was defined as the A/V ratio. The workflow for this software is presented in Figure 1.

Statistical Analysis

The results are expressed as the median (interquartile range) because, apart from age, all continuous data were not normally distributed (D'Agostino and Pearson normality test). Intergrader agreements (by two retinal specialists, A.I. and O.S.) in quantification of total, arterial-adjacent, and venous-adjacent nonperfusion area and A/V ratio were evaluated using the intraclass correlation coefficient (ICC) from 25 eyes in 12 × 12-mm images and 20 eyes in the montage images. The data were analyzed using the Kruskal-Wallis test followed by Dunn's multiple comparisons test to evaluate the differences among groups. Arterial-adjacent nonperfusion and venous-adjacent nonperfusion within each group was compared by the Wilcoxon matched-pairs signed rank test. The χ^2 test was used for categorical variables. Spearman's correlation coefficient was calculated to test the statistical correlation. Prism 7 (GraphPad Software, Inc., La Jolla, CA, USA) and SPSS v25 (SPSS, Inc., Chicago, IL, USA) were used for statistical analysis. A *P* value less than 0.05 was considered statistically significant.

RESULTS

Baseline Characteristics

Sixty-three eyes from 44 subjects (28 males and 16 females) were identified, and 40 eyes (64%) had FA images. Nine patients (20.5%) had type 1 diabetes while 35 patients (79.5%) had type 2 diabetes. Thirty-seven subjects (84.1%) also had hypertension. The median age of these subjects was 61 years (interquartile range, 51–68 years). The median duration of diabetes was 16 years (6–25 years), and the median hemoglobin A1c was 7.2% (6.7–9.0%). Of the 63 eyes, 22 were clinically graded as moderate NPDR, 16 as severe NPDR, and 25 as PDR. Ocular parameters and characteristics of the included eyes are shown in the Table. There were no significant differences among the groups with respect to BCVA, intraocular pressure, central macular thickness, presence of DME, or history of anti-VEGF treatment. Seventeen eyes (68.0%) with PDR had been treated with PRP.

Repeatability of the Quantitative Metrics

Because this study was a pilot analysis, intergrader agreements of the quantitative metrics were evaluated using ICC for 12 × 12-mm images and widefield montages, respectively. The ICCs (95% confidence interval) of total, arterial-adjacent, and venous-adjacent nonperfusion area, and A/V ratio were 0.986 (0.968–0.994), 0.767 (0.470–0.897), 0.823 (0.598–0.922), and 0.896 (0.765–0.954), respectively, for 12 × 12-mm OCTA images and 0.963 (0.907–0.985), 0.958 (0.893–0.983), 0.969 (0.922–0.988), and 0.934 (0.834–0.974), respectively, for widefield montages.

TABLE. Ocular Parameters and Characteristics of the Enrolled Eyes

	Moderate NPDR	Severe NPDR	PDR	*P* Value*
12 × 12-mm OCTA				
Eyes, *n*	22	16	25	
LogMAR visual acuity	0.24 (0.16–0.40)	0.30 (0.10–0.54)	0.18 (0.10–0.30)	0.5351
Intraocular pressure, mm Hg	15 (12–16)	15 (13–18)	16 (12–18)	0.3693
Central macular thickness, μm	245 (232–278)	270 (235–302)	262 (235–300)	0.3132
Macular edema, *n* (%)	8 (53%)	7 (44%)	7 (28%)	0.5781
Anti-VEGF injection, *n* (%)	4 (18%)	4 (25%)	11 (44%)	0.1371
PRP received, *n* (%)	–	–	17 (68%)	
Total nonperfusion area, %	3.49 (2.36–4.96)	6.69 (1.78–8.97)	8.59 (3.07–10.99)†	0.0073
Arterial-adjacent nonperfusion area, %	2.22 (1.50–3.13)	4.27 (1.23–5.92)	5.30 (2.16–6.78)†	0.0030
Venous-adjacent nonperfusion area, %	1.20 (0.57–1.74)	2.18 (0.61–3.16)	2.92 (1.17–5.10)†	0.0129
A/V ratio	1.93 (1.63–2.43)	1.86 (1.43–2.58)	1.78 (1.15–2.68)	0.5545
Widefield montage OCTA				
Eyes, *n*	9	11	17	
Log MAR visual acuity	0.30 (0.24–0.44)	0.30 (0.10–0.70)	0.18 (0.10–0.30)	0.1747
Intraocular pressure, mm Hg	12 (8–15)	15 (13–18)	17 (14–19)‡	0.0343
Central macular thickness, μm	249 (231–296)	258 (231–304)	264 (253–320)	0.5295
Macular edema, *n* (%)	3 (33%)	5 (45%)	4 (24%)	0.4976
Anti-VEGF injection, *n* (%)	2 (22%)	4 (36%)	8 (47%)	0.4589
PRP received, *n* (%)	–	–	17 (100%)	
Total nonperfusion area, %	5.18 (2.35–8.42)	10.72 (6.68–16.22)	13.85 (6.19–18.91)‡	0.0183
Arterial-adjacent nonperfusion area, %	3.38 (1.39–5.48)	6.58 (3.83–10.20)	9.38 (3.84–10.18)‡	0.0188
Venous-adjacent nonperfusion area, %	1.97 (0.97–3.42)	3.97 (2.84–7.11)	4.92 (2.55–8.59)‡	0.0189
A/V ratio	1.56 (1.44–2.31)	1.59 (1.27–1.84)	1.42 (1.18–1.95)	0.3509

All values are given as the median (interquartile range).
* Kruskal-Wallis test for continuous variables, and χ^2 test for categorical variables.
† Moderate NPDR versus PDR, $P < 0.01$, Dunn's multiple comparisons test.
‡ Moderate NPDR versus PDR, $P < 0.05$, Dunn's multiple comparisons test.

Nonperfusion Adjacency to Arteries or Veins in 12 × 12-mm OCTA

The summary of the results is also shown in the Table. In the macular 12 × 12-mm OCTA images, the median total nonperfusion area was 3.49% in moderate NPDR, 6.62% in severe NPDR, and 8.56% in PDR. There was a significant difference in nonperfusion between the moderate NPDR and PDR groups ($P < 0.001$). Arterial-adjacent nonperfusion and venous-adjacent nonperfusion had the same trends as total nonperfusion: Both increased with increasing DR severity, and significant difference was observed only between the moderate NPDR and PDR groups. In all stages, arterial-adjacent nonperfusion was significantly larger than venous ($P < 0.001$ for all stages).

The median A/V ratios were 1.93 in moderate NPDR, 1.84 in severe NPDR and 1.78 in PDR. There was no significant difference among the groups ($P = 0.49$). However, when A/V ratios were plotted against total nonperfusion, there was a negative correlation ($r = -0.600$, 95% confidence interval: -0.742 to -0.408, $P < 0.0001$, Fig. 2).

Nonperfusion Adjacency to Arteries or Veins in Widefield Montages

In 37 eyes (9 eyes with moderate NPDR, 11 eyes with severe NPDR, and 17 eyes with PDR), widefield montages were also taken. The results are also shown in the Table and followed the same trends seen in the central 12 × 12-mm images: The total
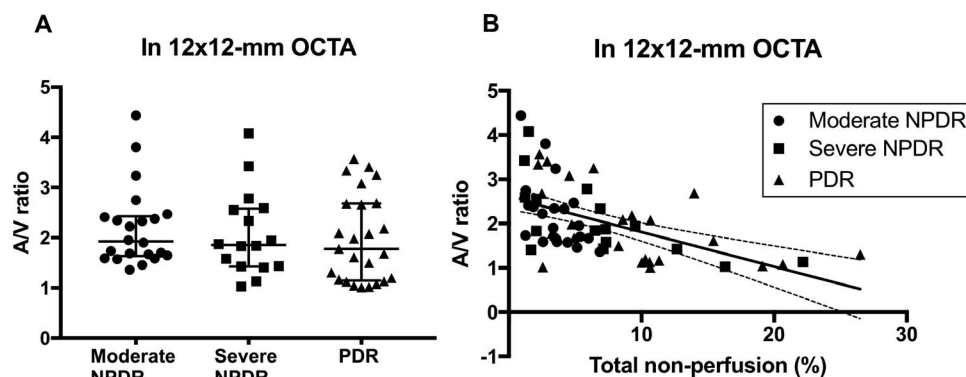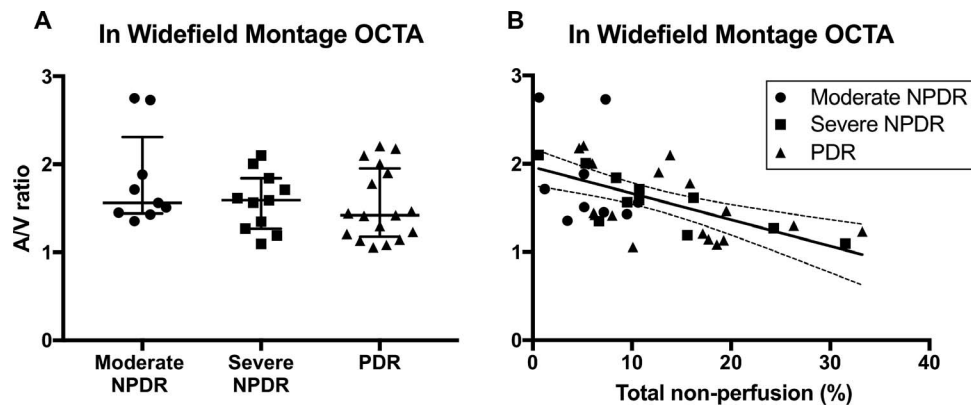

FIGURE 2. Individual plots of the ratios of arterial-adjacent versus venous-adjacent nonperfusion (A/V ratios) in the eyes with moderate NPDR, severe NPDR, and PDR in 12 × 12-mm OCTA images. *Lines* are at the median with interquartile range. **(A)** A/V ratios tend to decrease with increasing DR severity, but there is no significant difference among the stages. **(B)** When each A/V ratio is plotted against the total nonperfusion percentage in each eye, the ratio is negatively correlated with the total nonperfusion ($r = -0.600$, 95% confidence interval: -0.742 to -0.408, $P < 0.0001$).

FIGURE 3. Individual plots of the ratios of arterial-adjacent versus venous-adjacent nonperfusion (A/V ratios) in the eyes with moderate NPDR, severe NPDR, and PDR in widefield montages. (**A**) A/V ratios tend to decrease with increasing DR severity, but there is no significant difference among the stages. The behavior of the A/V ratio is the same as in 12×12-mm images (Fig. 2), but the ratios are smaller than in 12×12-mm images. (**B**) The A/V ratio is negatively correlated with the total nonperfusion percentage ($r = -0.598$, 95% confidence interval: -0.777 to -0.332, $P < 0.0001$).

nonperfusion, arterial-adjacent nonperfusion, and venous-adjacent nonperfusion gradually increased with increasing DR severity, and only the difference between the moderate NPDR and PDR groups reached significance. The A/V ratios in the montage images were positively correlated with those in the 12×12-mm images ($r = 0.691$, 95% confidence interval: 0.465–0.832, $P < 0.0001$), but were smaller than in the 12×12-mm images. The median A/V ratio was 1.56 in moderate NPDR, 1.59 in severe NPDR, and 1.42 in PDR. The A/V ratio for the montage images was also negatively correlated with the total nonperfusion ($r = -0.598$, 95% confidence interval: -0.777 to -0.332, $P < 0.0001$, Fig. 3).

Case Presentation

Representative cases are shown in Figures 4 and 5. The total nonperfusion in 12×12-mm images from the left eye of a 75-year-old male with moderate NPDR was 1.28%, and the A/V ratio was 2.75. Small nonperfusion areas were clearly located adjacent to the retinal arterial branches (Fig. 4). On the other hand, in the right eye of a 34-year-old male with severe NPDR, the total nonperfusion in his montage was 10.72%, and the A/V ratio was 1.59. Small nonperfusion areas also tended to be observed adjacent to the arterial side. However, some severely enlarged nonperfusion areas in the outside arcade extended toward the venous side (Fig. 5). Sparse and irregular capillaries near the venous side were residually observed.

DISCUSSION

OCTA can detect flow signals with high contrast, thus visualizing nonflow areas (i.e., nonperfusion areas) at the capillary level. Recent studies using OCTA as well as FA have quantitatively evaluated capillary nonperfusion areas in DR, and have generally demonstrated that capillary nonperfusion increases with increasing DR severity.[13,20,21] The results herein agree with these findings (Table). Furthermore, compared to FA, OCTA can also visualize periarterial capillary-free zones[16–18] and vessel connections at the level of precapillary arterioles and venules. These advantages enabled us to identify and trace small branches of arteries and veins on OCTA images. Using a computer-based algorithm to determine the shortest distance from the vessels, we evaluated nonperfusion adjacency to the arterial side or the venous side automatically and quantitatively.

This OCTA pilot analysis revealed two major findings for nonperfusion adjacency in DR. First, capillary nonperfusion adjacent to the arterial side was larger than to the venous side in all DR stages (Table). The eyes in which smaller nonperfusion areas were detected tended to have larger A/V ratios without any regard to the level of DR severity (Figs. 2–4). These results indicate that diabetic capillary nonperfusion may begin developing near the arterial side. Previous histologic studies, which have found that arterial-side vascular involvement is implicated in the pathogenesis of the diabetic microvascular lesions, support this observation. Basement membrane thickening, which could be responsible for endothelial–pericyte miscommunication, was mostly observed in capillaries associated with an arterial environment compared to those in a venous environment in postmortem diabetic human[4] and experimental dog[6] eyes. Also, it was histologically reported that microaneurysms occurred largely on the arterial side,[7] and regions of acellular capillaries corresponding to nonperfusion were often observed downstream from the areas where precapillary arterioles had severe loss of smooth muscle cells in their walls.[8,9] Impairment of autoregulation owing to pericyte and smooth muscle cell loss in the arterial vasculature could induce intraluminal focal hypertension and mechanical high shear stress in the arterial side of capillary bed; these have been implicated as contributory factors in the formation of not only basement membrane thickening and microaneurysms but also acellular capillaries resulting from endothelial cell death.[6–9] The current results from OCTA images provide an estimate of the arterial-side vascular involvement in the initiation of retinal microvascular abnormalities in DR.

The second major finding was that the A/V ratio for capillary nonperfusion decreased and approached 1.0 with increasing nonperfusion (Figs. 2, 3). This suggests that the capillary nonperfusion in DR could be enlarging from the arterial side toward the venous side with disease progression. This finding could be consistent with known diabetic pathophysiologic changes, which could let us estimate the mechanisms of enlarging the nonperfusion. In particular, using experimental diabetic models, leukostasis has also been identified as one of the important factors in forming obliterated and/or acellular capillaries.[22–25] Moreover, it has been reported that leukostasis is more likely to occur on the venous side because veins have passive flow, and leukocytes tend to move closer to the endothelial surface in veins than in the central arterial bloodstream.[25,26] Early in disease progression, the
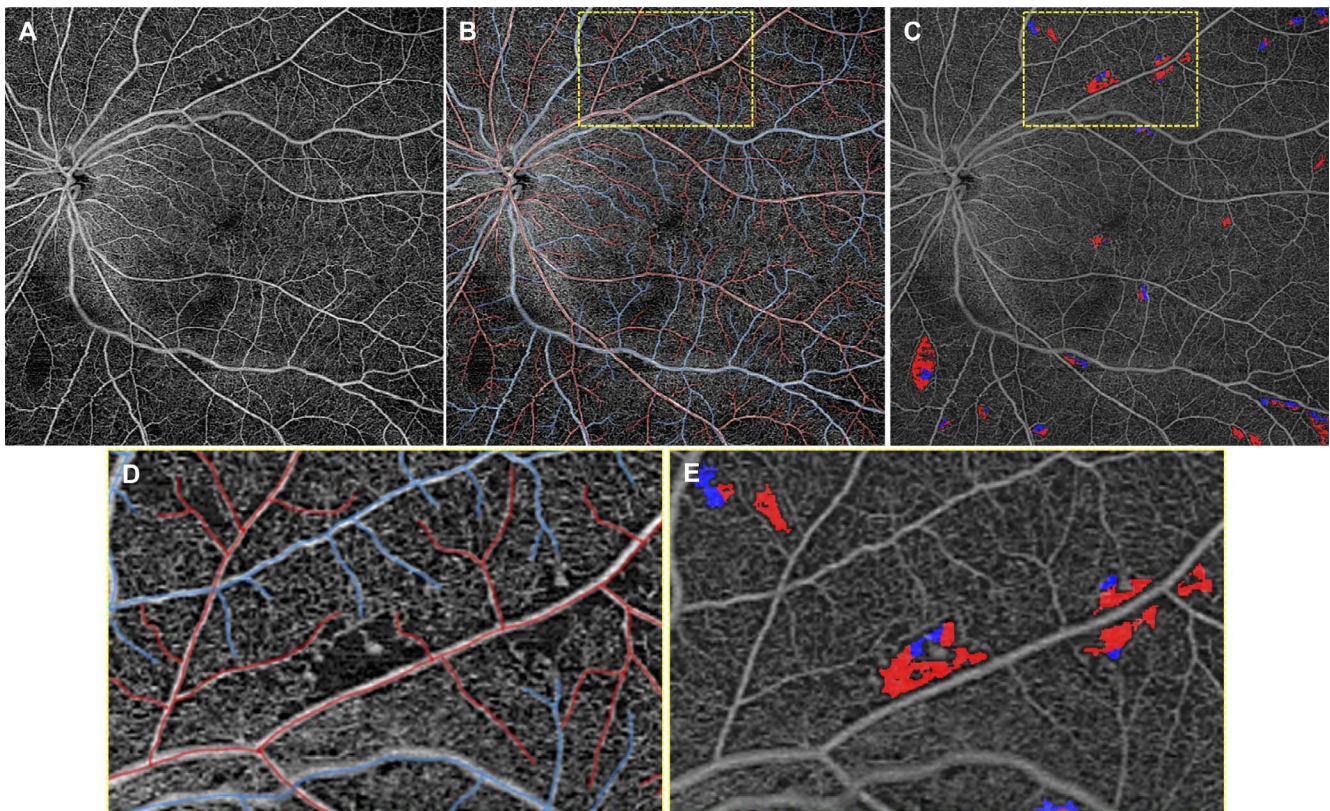
FIGURE 4. A 75-year-old male with moderate NPDR and small capillary nonperfusion areas. (**A**) The original 12 × 12-mm OCTA image of the full retinal thickness. Small nonperfusion areas are sparsely distributed. (**B**) An image showing arteries traced as *red* and veins traced as *blue*. The *yellow rectangle* is zoomed in the *bottom row* (**D**, **E**). (**C**) The percentage of detected capillary nonperfusion of the eye is 1.28%. According to the traced images, the software displays the arterial-adjacent nonperfusion as red pixels, and venous-adjacent nonperfusion as blue pixels. The arterial/venous nonperfusion ratio was 2.75. (**D**) Magnified image showing small nonperfusion areas located adjacent to the retinal arterial branches. (**E**) Using the software, *red areas* that display the arterial-adjacent nonperfusion are predominantly observed.

arterial vascular damage reduces perfusion to the downstream venous-side capillaries. Hypoxia from hypoperfusion causes upregulation of proangiogenic factors such as VEGF in retinal tissues, which promotes leukocyte adhesion and thus increased leukostasis.[27,28] Leukostasis in turn exacerbates endothelial damage, resulting in increased formation of acellular capillaries and the enlargement of capillary nonperfusion toward the venous side.

In addition, we found that the capillary nonperfusion A/V ratio in the montage images was negatively correlated with the total nonperfusion, and the ratios were smaller than those in the 12 × 12-mm images (Fig. 3). This could be partially explained by the fact that total nonperfusion detected in the montage images was larger than that in 12 × 12-mm images (Table) because the majority of the capillary nonperfusion in DR occurs outside of the macular region.[29–31] The peripheral capillary nonperfusion also tended to be found in larger patches, and was more commonly enlarged toward the venous side (Fig. 5).

Recently, other studies have focused on the distribution of retinal ischemia in other diseases in order to assess pathophysiology. Several studies examined patterns of retinal ischemia in paracentral acute middle maculopathy (PAMM) due to retinal vascular diseases using en face OCT.[32,33] In PAMM due to a branch artery occlusion, band-like hyperreflective ischemic lesions in the middle retina on en face OCT were shown to occur on the arteriolar sides, as expected.[32] On the other hand, Ghasemi Falavarjani et al.[33] demonstrated that ischemic changes always occurred on the venous side in PAMM due to retinal vein occlusion, and hypothesized that impaired arterial

perfusion secondary to high venous pressure gradient could strongly affect the circulation of perivenular tissues that were farthest from arterial circulation. Taken together with our findings, this suggests that, although both DR and retinal vein occlusion induce retinal ischemia, the ischemic patterns appear to be different. Therefore, a greater knowledge of capillary nonperfusion adjacency to the arterial side or venous side would contribute to understanding the etiology of other retinal vascular diseases. The current pilot study was for DR only, so further studies are needed to investigate the characteristics of the retinal ischemia in other retinal diseases.

The current results could also be linked to the origins of neovascularization elsewhere (NVE) and intraretinal microvascular abnormalities (IRMAs) reported most recently by Pan et al.[34] using OCTA in PDR eyes. They classified NVEs into three types: originating from the venous side, capillary networks, and IRMAs. They also reported that IRMAs originated from and drained into retinal venules. Our results indicated that capillary nonperfusion could progress from the arterial side toward the venous side. In addition, we visualized sparse but residual capillaries within venous-side nonperfusion, but few on the arterial side (Fig. 5). These residual capillaries may be remodeled into IRMAs, and may induce the formation of NVEs that breach the internal limiting membrane, as reported previously.[35] Our observation could partially explain the reason why NVEs and IRMAs predominantly originate near the venous side.

This study has several limitations. First, we focused on relatively advanced DR in the current study; thus, the differences in nonperfusion areas reached significance only
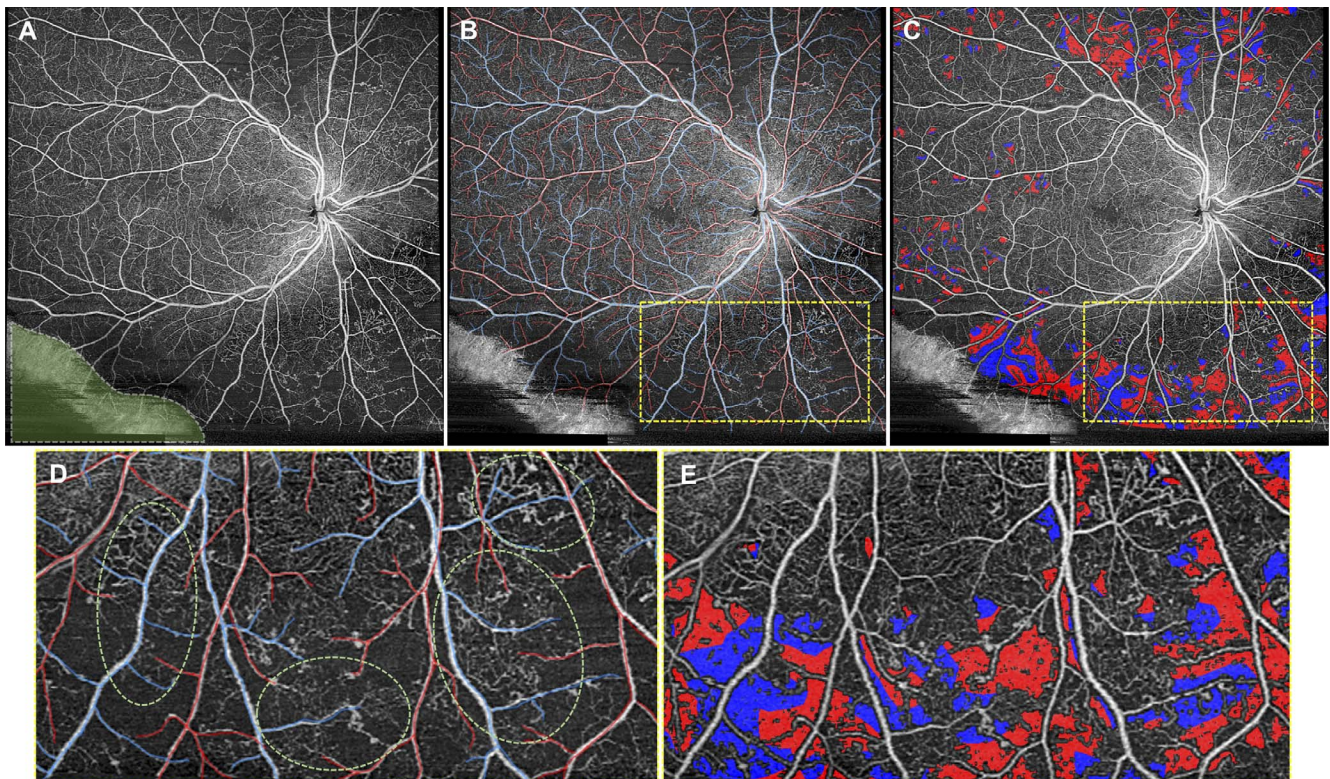
FIGURE 5. A 34-year-old male with severe NPDR and large capillary nonperfusion areas. (A) The original widefield montage of whole retina. Large nonperfusion areas are distributed mainly outside the arcade. The *green part* at the *bottom left corner* has a segmentation artifact and is removed before nonperfusion areas are detected. (B) An image showing arteries traced as *red* and veins traced as *blue*. The *yellow rectangle* is zoomed in the *bottom row* (D, E). (C) The percentage of detected capillary nonperfusion of the eye is 10.72%. According to the traced images, the software displays the arterial-adjacent nonperfusion as red pixels, and venous-adjacent nonperfusion as blue pixels. The arterial/venous nonperfusion ratio is 1.59. As in Figure 4, small nonperfusion areas tend to be observed adjacent to arterial side; however, some severely enlarged nonperfusion areas in the outer arcade extend toward the venous side. (D) Magnified image showing sparse and irregular residual capillaries near the venous side (*green dot ellipses*). (E) *Blue areas* that display the venous-adjacent nonperfusion areas are more prominent compared to Figure 4.

between moderate NPDR and PDR (Table). Moreover, the interquartile ranges were rather wide in each stage. Therefore, the nonperfusion area may not be linearly correlated to the advanced DR stages, which are diagnosed from ophthalmoscopic findings such as the presence of IRMA and neovascularization. Also, since the A/V ratio was negatively and significantly correlated with the total nonperfusion area (Figs. 2B, 3B), the A/V ratio in the nonperfusion area was variant within the stages and had no significant difference among the stages. These results suggest that A/V ratio may not have enough power to differentiate between DR stages, especially in severe cases, but is more helpful as a metric for understanding how the capillary nonperfusion enlarges. This was also a pilot study, cross-sectionally recruiting patients with NPDR and PDR. Future prospective studies should be performed that follow up on the same eyes with and without DR longitudinally to more precisely elucidate the progression of diabetic retinal ischemia. Second, we cannot exclude the combined effect of hypertension in analyzing nonperfusion adjacency because 84.1% of recruited patients had hypertension. To strictly exclude the effects from such systemic factors, only patients with type 1 diabetes mellitus and no other systemic diseases would need be recruited. Third, we included eyes that had previously been treated with anti-VEGF injections and PRP. A retrospective analysis of RISE and RIDE reported decreased rates of progression of nonperfusion in patients treated with ranibizumab,[36] and it has been reported using widefield FA that anti-VEGF injections lead to reperfusion in areas of capillary dropout in DR.[37] On the other hand, previous studies have

suggested that there are no significant differences in macular vascular densities before and after anti-VEGF therapy for DME observed using OCTA.[38,39] Furthermore, a recent prospective study revealed that OCTA parameters (foveal avascular zone, and superficial/deep capillary densities) were not significantly affected by PRP.[40] Although FA is the gold standard for evaluating peripheral retinal nonperfusion, fluorescein leakage and photocoagulation scars interfere with the observation of the retinal nonperfusion area after PRP. Even though the current study did not include the eyes immediately after the therapies (anti-VEGF injection and/or PRP within 3 months), the possible effects of the therapies on the retinal nonperfusion should be considered. Further studies using OCTA are needed to investigate completely treatment-naïve retinal nonperfusion and to verify whether reperfusion occurs predominantly on the arterial or venous side after these therapies. Lastly, we also included patients with DME, which may have altered OCTA imaging and quantification. However, since DME would be expected to most significantly impact only the macular region of the image, this likely would have had a small effect on quantification of large widefield montage images.

There were also several limitations in terms of our image analysis methodology. As mentioned previously, OCTA visualizes a narrow capillary-free zone that physiologically exists around retinal arteries.[16–18] Automated quantification could erroneously detect this physiologic zone as a nonperfusion area, and the A/V ratio could have been overestimated because the periarterial physiologic capillary-free zones could still

contribute to nonperfusion areas when combined with actual areas of nonperfusion in eyes with DR. However, we confirmed manually that this physiologic capillary-free zone was not detected as areas of nonperfusion by our software in eyes without DR.[13] Moreover, a very recent study quantitatively demonstrated that the periarterial capillary-free zone in severe NPDR was enlarged compared to that in the normal subjects.[41] As shown in Figure 4, our software was also able to estimate that early nonperfusion areas in DR occurred by enlargement of this capillary-free zone. Indeed, we cannot separate physiologic capillary-free zone from the pathologically enlarged nonperfusion area in en face OCTA images.

If the current method can be modified to subtract physiologic capillary-free zone around retinal arteries from the area defined as nonperfusion, it could result in a more accurate representation of the A/V ratio. Another limitation of our analysis was that we used only OCTA images of the full retinal thickness. In the PDR eyes, NVEs are projected toward deeper retinal structures, so the capillary nonperfusion areas, especially those adjacent to the venous side near the NVEs, were inevitably underestimated. Moreover, we did not assess the spatial difference in nonperfusion adjacency to arteries or veins between the superficial and deep retinal capillary layers. Because the majority of retinal nonperfusion was reported outside of the macular region,[29–31] we used the 12 × 12-mm images; however, the lower resolution of these larger images prevented investigation of the deep plexus. Nonperfusion of the deep plexus can occur in regions with relatively intact overlying superficial plexus.[42] Thus, the nonperfusion areas could be underestimated. To prevent this, creating a montage from smaller images with higher resolution may be useful in future studies. Moreover, subtle differences in alignment between scans may have caused variation in measurements from eye to eye.

In summary, the current pilot study using widefield OCTA images suggests that nonperfusion in DR may distribute predominantly near arteries, and, with increasing size, extend toward veins. This approach could provide new insights for assessing the pathogenesis of retinal vascular diseases.

References

1. Antonetti DA, Klein R, Gardner TW. Diabetic retinopathy. *N Eng J Med*. 2012;366:1227–1239.

2. Duh EJ, Sun JK, Stitt AW. Diabetic retinopathy: current understanding, mechanisms, and treatment strategies. *JCI Insight*. 2017;2:e93751.

3. Ashton N. Arteriolar involvement in diabetic retinopathy. *Br J Ophthalmol*. 1953;37:282–292.

4. Ashton N. Vascular basement membrane changes in diabetic retinopathy. Montgomery lecture, 1973. *Br J Ophthalmol*. 1974;58:344–366.

5. Garner A. Histopathology of diabetic retinopathy in man. *Eye (Lond)*. 1993;7(pt 2):250–253.

6. Stitt AW, Anderson HR, Gardiner TA, Archer DB. Diabetic retinopathy: quantitative variation in capillary basement membrane thickening in arterial or venous environments. *Br J Ophthalmol*. 1994;78:133–137.

7. Stitt AW, Gardiner TA, Archer DB. Histological and ultrastructural investigation of retinal microaneurysm development in diabetic patients. *Br J Ophthalmol*. 1995;79:362–367.

8. Gardiner TA, Archer DB, Curtis TM, Stitt AW. Arteriolar involvement in the microvascular lesions of diabetic retinopathy: implications for pathogenesis. *Microcirculation*. 2007; 14:25–38.

9. Curtis TM, Gardiner TA, Stitt AW. Microvascular lesions of diabetic retinopathy: clues towards understanding pathogenesis? *Eye (Lond)*. 2009;23:1496–1508.

10. Spaide RF, Fujimoto JG, Waheed NK, Sadda SR, Staurenghi G. Optical coherence tomography angiography. *Prog Retin Eye Res*. 2018;64:1–55.

11. Kashani AH, Chen CL, Gahm JK, et al. Optical coherence tomography angiography: a comprehensive review of current methods and clinical applications. *Prog Retin Eye Res*. 2017; 60:66–100.

12. Ishibazawa A, Nagaoka T, Takahashi A, et al. Optical coherence tomography angiography in diabetic retinopathy: a prospective pilot study. *Am J Ophthalmol*. 2015;160:35–44, e31.

13. Alibhai AY, De Pretto LR, Moult EM, et al. Quantification of retinal capillary nonperfusion in diabetics using wide-field optical coherence tomography angiography [published online ahead of print December 18, 2018]. *Retina*. doi:10.1097/IAE.0000000000002403.

14. Wilkinson CP, Ferris FL III, Klein RE, et al. Proposed international clinical diabetic retinopathy and diabetic macular edema disease severity scales. *Ophthalmology*. 2003;110: 1677–1682.

15. Sawada O, Ichiyama Y, Obata S, et al. Comparison between wide-angle OCT angiography and ultra-wide field fluorescein angiography for detecting non-perfusion areas and retinal neovascularization in eyes with diabetic retinopathy. *Graefes Arch Clin Exp Ophthalmol*. 2018;256:1275–1280.

16. Mase T, Ishibazawa A, Nagaoka T, Yokota H, Yoshida A. Radial peripapillary capillary network visualized using wide-field montage optical coherence tomography angiography. *Invest Ophthalmol Vis Sci*. 2016;57:OCT504–OCT510.

17. Coscas G, Lupidi M, Coscas F, Chhablani J, Cagini C. Optical coherence tomography angiography in healthy subjects and diabetic patients. *Ophthalmologica*. 2018;239:61–73.

18. Balaratnasingam C, An D, Sakurada Y, et al. Comparisons between histology and optical coherence tomography angiography of the periarterial capillary-free zone. *Am J Ophthalmol*. 2018;189:55–64.

19. Maurer C, Qi R, Raghavan V. A linear time algorithm for computing exact Euclidean distance transforms of binary images in arbitrary dimensions. *IEEE Trans Pattern Anal Mach Intell*. 2003;25:265–270.

20. Schottenhamml J, Moult EM, Ploner S, et al. An automatic, intercapillary area-based algorithm for quantifying diabetes-related capillary dropout using optical coherence tomography angiography. *Retina*. 2016;36(suppl 1):S93–S101.

21. Hwang TS, Hagag AM, Wang J, et al. Automated quantification of nonperfusion areas in 3 vascular plexuses with optical coherence tomography angiography in eyes of patients with diabetes. *JAMA Ophthalmol*. 2018;136:929–936.

22. Joussen AM, Murata T, Tsujikawa A, Kirchhof B, Bursell SE, Adamis AP. Leukocyte-mediated endothelial cell injury and death in the diabetic retina. *Am J Pathol*. 2001;158:147–152.

23. Joussen AM, Poulaki V, Qin W, et al. Retinal vascular endothelial growth factor induces intercellular adhesion molecule-1 and endothelial nitric oxide synthase expression and initiates early diabetic retinal leukocyte adhesion in vivo. *Am J Pathol*. 2002;160:501–509.

24. Kern TS. Contributions of inflammatory processes to the development of the early stages of diabetic retinopathy. *Exp Diabetes Res*. 2007;2007:95103.

25. Tsujikawa A, Ogura Y. Evaluation of leukocyte-endothelial interactions in retinal diseases. *Ophthalmologica*. 2012;227:68–79.

26. Granger DN, Kubes P. The microcirculation and inflammation: modulation of leukocyte-endothelial cell adhesion. *J Leukoc Biol*. 1994;55:662–675.

27. Liu Y, Cox SR, Morita T, Kourembanas S. Hypoxia regulates vascular endothelial growth factor gene expression in endothelial cells. Identification of a 5′ enhancer. *Circ Res*. 1995;77:638–643.

28. Takagi H, King GL, Ferrara N, Aiello LP. Hypoxia regulates vascular endothelial growth factor receptor KDR/Flk gene expression through adenosine A2 receptors in retinal capillary endothelial cells. *Invest Ophthalmol Vis Sci*. 1996;37:1311–1321.

29. Niki T, Muraoka K, Shimizu K. Distribution of capillary nonperfusion in early-stage diabetic retinopathy. *Ophthalmology*. 1984;91:1431–1439.

30. Shimizu K, Kobayashi Y, Muraoka K. Midperipheral fundus involvement in diabetic retinopathy. *Ophthalmology*. 1981;88:601–612.

31. Silva PS, Dela Cruz AJ, Ledesma MG, et al. Diabetic retinopathy severity and peripheral lesions are associated with nonperfusion on ultrawide field angiography. *Ophthalmology*. 2015;122:2465–2472.

32. Sridhar J, Shahlaee A, Rahimy E, et al. Optical coherence tomography angiography and en face optical coherence tomography features of paracentral acute middle maculopathy. *Am J Ophthalmol*. 2015;160:1259–1268.

33. Ghasemi Falavarjani K, Phasukkijwatana N, Freund KB, et al. En face optical coherence tomography analysis to assess the spectrum of perivenular ischemia and paracentral acute middle maculopathy in retinal vein occlusion. *Am J Ophthalmol*. 2017;177:131–138.

34. Pan J, Chen D, Yang X, et al. Characteristics of neovascularization in early stages of proliferative diabetic retinopathy by optical coherence tomography angiography. *Am J Ophthalmol*. 2018;192:146–156.

35. Lee CS, Lee AY, Sim DA, et al. Reevaluating the definition of intraretinal microvascular abnormalities and neovascularization elsewhere in diabetic retinopathy using optical coherence tomography and fluorescein angiography. *Am J Ophthalmol*. 2015;159:101–110.

36. Campochiaro PA, Wykoff CC, Shapiro H, Rubio RG, Ehrlich JS. Neutralization of vascular endothelial growth factor slows progression of retinal nonperfusion in patients with diabetic macular edema. *Ophthalmology*. 2014;121:1783–1789.

37. Levin AM, Rusu I, Orlin A, et al. Retinal reperfusion in diabetic retinopathy following treatment with anti-VEGF intravitreal injections. *Clin Ophthalmol*. 2017;11:193–200.

38. Mane V, Dupas B, Gaudric A, et al. Correlation between cystoid spaces in chronic diabetic macular edema and capillary nonperfusion detected by optical coherence tomography angiography. *Retina*. 2016;36(suppl 1):S102–S110.

39. Ghasemi Falavarjani K, Iafe NA, Hubschman JP, Tsui I, Sadda SR, Sarraf D. Optical coherence tomography angiography analysis of the foveal avascular zone and macular vessel density after anti-VEGF therapy in eyes with diabetic macular edema and retinal vein occlusion. *Invest Ophthalmol Vis Sci*. 2017;58:30–34.

40. Lorusso M, Milano V, Nikolopoulou E, et al. Panretinal photocoagulation does not change macular perfusion in eyes with proliferative diabetic retinopathy. *Ophthalmic Surg Lasers Imaging Retina*. 2019;50:174–178.

41. Li H, Ding X, Lu L, Yang J, Ma J. Morphometry of the normal retinal periarteral capillary-free zone and changes during severe nonproliferative diabetic retinopathy. *Clin Hemorheol Microcirc*. 2019;72:169–178.

42. Scarinci F, Nesper PL, Fawzi AA. Deep retinal capillary nonperfusion is associated with photoreceptor disruption in diabetic macular ischemia. *Am J Ophthalmol*. 2016;168:129–138.